Excellent Tunable DC Bias Superposition Characteristics for Manganese–Zinc Ferrites

Guohua Wu, Zhong Yu, Ke Sun, *Member, IEEE*, Rongdi Guo, Bo Wang, Xiaona Jiang, Lezhong Li, and Zhongwen Lan

***Abstract*—Manganese–zinc (MnZn) power ferrites own significant applications in inductors and transformers for power conversion. The performance of these components is dependent on permeability, saturation induction, core losses, and dc bias superposition characteristics of MnZn ferrites. It is worth emphasizing that excellent dc bias superposition characteristics of ferrites are beneficial for the stability and efficiency of power converters operated with both ac and dc signals. In this paper, Co_2O_3-doped MnZn ferrites are fabricated using a solid-state reaction method and used to investigate dc bias superposition characteristics of permeability and core losses. More importantly, the physical mechanism of the dc bias superposition characteristics is clarified. Furthermore, the effect of Co_2O_3 doping on the efficiency of buck circuit was also investigated. The dc bias superposition characteristics suggests potential application in power components and systems.**

***Index Terms*—Core losses, dc bias superposition, MnZn ferrites, permeability.**

I. Introduction

In VIRTUE of high saturation magnetic induction (B_s), high initial permeability (μ_i), and low core losses (P_L), manganese–zinc (MnZn) ferrites have been used as transformer cores in numerous convertors and switching mode power supplies [1]–[3]. However, magnetic components with dc currents experience deteriorated material properties like increased core losses. This reduces the stability and efficiency of the power converters [4]–[6]. Therefore, the physical mechanism of the dc bias superposition characteristics of MnZn ferrites needs to be investigated, to improve the stability and efficiency of power conversion devices. The quality of the dc bias superposition characteristics for power ferrites has largely been determined using permeability and core losses in the literature [7]–[17].

Permeability of dc bias superposition characteristics in low-loss MnZn ferrite cores working at frequency higher than 3 MHz has been reported to remain at a constant value, and gradually decreases with an increase of dc bias field (H_{dc}) [7], [8]. NiZn ferrites with fine microstructure and small grains have better dc bias superposition characteristic of permeability, due to higher ΔB ($\Delta B = B_s - B_r$, where B_r is remanent induction) approximately 163 mT [9]. Homoplastically, the composite additives of 2.0 wt% Bi_2O_3, 1.5 wt% AlBSi glass, and 1.5 wt% SnO_2 can achieve a small grain size D (1–2 μm) for averting the reduction of permeability under dc bias superposition [10]. Furthermore, Fe^{2+} ions in MnZn ferrites are beneficial for steady permeability under dc bias superposition, due to the uniaxial anisotropy induced by Fe^{2+} ions, restricting the movement of domain wall [11]. Overall, these works suggest that fine microstructure, small grain size, and suitable additives improve the dc bias superposition characteristic of permeability. Small grain size would reduce permeability.

The core loss in dc bias superposition varies as the dc bias field differs in terms of the material stoichiometrics and measurement techniques [12], [15], [17]. To address the difficulty in measuring core losses in ferrite, an accurate circuit to evaluate the core losses under dc bias superposition is reported [12]. Core losses of MnZn ferrites under low ac excitation (<200 kHz) and high dc bias excitation monotonically increase with an increase in dc bias field [5], [13], [14]. In low-temperature cofired ceramic materials, core losses do not monotonically increase with dc bias field, but show a minimum value [15], [16]. A similar variation in core losses has been reported for MnZn ferrites in a study using a Steinmetz premagnetization graph to calculate the core losses under dc bias superposition [17]. However, to the best of the authors knowledge there is no theory that interprets dc bias superposition characteristic of core losses, restricting the development of low-loss ferrite cores under dc bias.

To date, reported studies investigating the dc bias superposition characteristics do not reveal a physical mechanism. This paper addresses the shortcoming by investigating the physical mechanism of dc bias superposition characteristics in MnZn ferrites. Referring to [18], strong magnetic anisotropy is beneficial for maintaining permeability under dc bias field. In this paper, Co^{2+} ions, with stronger uniaxial anisotropy than Fe^{2+} ions, were used in MnZn ferrites to improve the dc bias superposition characteristics of permeability. In addition, based on technical magnetization theory, the effect of dc bias field on permeability was investigated in detail. Separation method of core losses enables the effect of dc bias field on hysteresis loss (P_h), eddy current loss (P_e), and residual loss (P_r) to be investigated. DC

Manuscript received December 5, 2018; revised April 14, 2019; accepted May 27, 2019. Date of publication June 9, 2019; date of current version November 12, 2019. This work was supported by the National Natural Science Foundation of China under Grants 51472045 and 51772046. Recommended for publication by Associate Editor Dr. Juan Rivas Davila. *(Corresponding author: Ke Sun.)*

G. Wu, Z. Yu, K. Sun, R. Guo, B. Wang, X. Jiang, and Z. Lan are with the School of Materials and Energy, University of Electronic Science and Technology of China, Chengdu 610054, China (e-mail: 657669389@qq.com; yuzhong@uestc.edu.cn; ksun@uestc.edu.cn; guorongdi@uestc.edu.cn; 809967953@qq.com; xnjiang@uestc.edu.cn; zwlan@uestc.edu.cn).

L. Li is with the Sichuan Province Key Laboratory of Information Materials and Devices Application, Chengdu University of Information Technology, Chengdu 610225, China (e-mail: lezhongli@cuit.edu.cn).

Color versions of one or more of the figures in this paper are available online at http://ieeexplore.ieee.org.

Digital Object Identifier 10.1109/TPEL.2019.2921868

bias field did not just monotonically deteriorate the magnetic property of ferrite core, but also increase the permeability and reduce the core losses. This finding suggests a novel way for optimizing dc bias superposition characteristics in power ferrites. In addition, in a buck circuit, the 0.30 wt% Co_2O_3 sample improved the efficiency of circuit.

II. Experimental Procedures

MnZn ferrite cores with an optimized iron-rich composition of $Mn_{0.67}Zn_{0.21}Fe_{2.12}O_4$ were produced by solid-state reaction method. The excess Fe_2O_3 formed Fe_3O_4 during the sintering process, which decreased the magneto-crystalline anisotropy constant (K_1) [19]. However, excess Fe_3O_4 also reduced the resistivity of the bulk material. Based on the optimized composition, the MnZn ferrite samples should have high resistivity and low core losses at high-frequency range. After being accurately weighed, highly purified (>99.7 wt%) powder of Fe_2O_3, Mn_3O_4, and ZnO was mixed homogeneously at 241 r/min for 2 h using a planetary mill. The milling media was zirconia balls and deionized water. After oven drying at 100 °C for 20 h, the mixtures were calcined in air at 910 °C for 2 h in an elevator furnace. The additives 0.00–0.35 wt% Co_2O_3, 0.10 wt% $CaCO_3$, 0.03 wt% V_2O_5, 0.20 wt% TiO_2, and 0.06 wt% SnO_2 were added to the calcined powder. The amount of additives was selected to refine the grains during the sintering process and enhance the resistivity of the bulk material. After milling in planetary mill at 241 r/min for 4 h, the dried powder was granulated using 13 wt% poly-vinyl alcohol. The granules were then pressed under 6 MPa into toroidal cores, having dimensions of 18-mm outer diameter, 8-mm inner diameter, and 5-mm thickness. Finally, the toroidal cores were sintered in a tube furnace at 1150 °C for 6 h with 5% oxygen.

Scanning electron microscopy (SEM, JEOL JSM-6490LV) was used to observe the microstructure of the fracture surface. Average grain size D was measured through interception method. B–H analyzer (IWATSU SY-8232) was used to determine core losses and hysteresis loops. The permeability and resistivity were determined using the inductance and resistance, respectively, which were performed by a *LCR* digital electric bridge (Tonghui TH2826). DC bias superposition characteristics were measured using the circuit model shown in Fig. 1. N_1 and N_2 were windings for test ports, and N_3 was extra winding for adding an adjustable dc source (I_{dc}) to provide a dc bias field along the magnetic path of the toroidal core. The value H_{dc} was calculated using the following equation [6]:

$$H_{dc} = N_3 I_{dc} / l_e \tag{1}$$

where l_e is the effective length of the toroidal core. To restrain the ac signal induced by the test ports in N_3, a large inductance L of 20 mH was selected. The resistance (R) of ferrite sheet under different H_{dc} was measured, as shown in Fig. 2, where H_{dc} is perpendicular to the plane of the magnetic sheet. Furthermore, to investigate the effect of manufactured ferrite core on the performance of circuit, the ferrite cores were used in the inductor L_C in a buck circuit, where synchronous MOSFETs was used, as shown in Fig. 3. The input capacitance C_{IN} and output

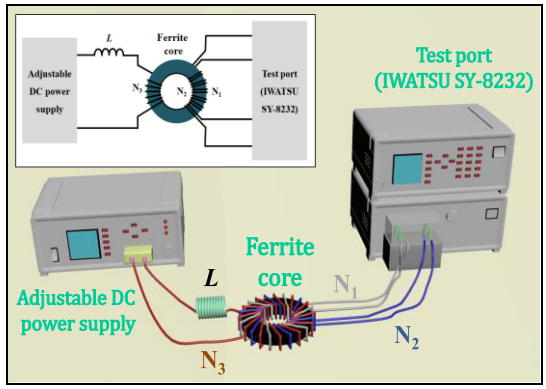

(a)

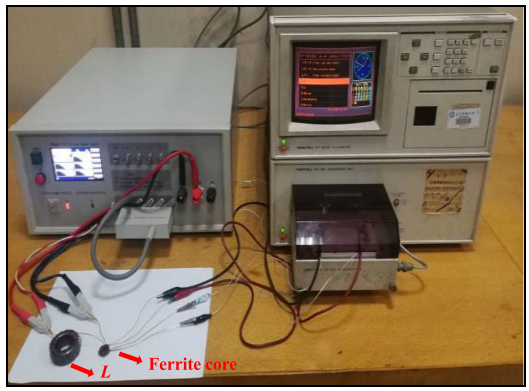

(b)

Fig. 1. (a) The circuit model and (b) measuring setup of dc bias superposition.

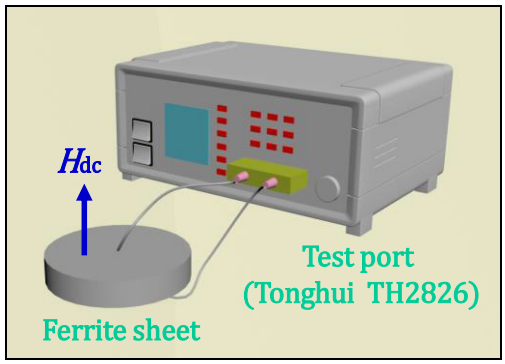

Fig. 2. A sketch of the circuit for measuring resistance under different H_{dc}.

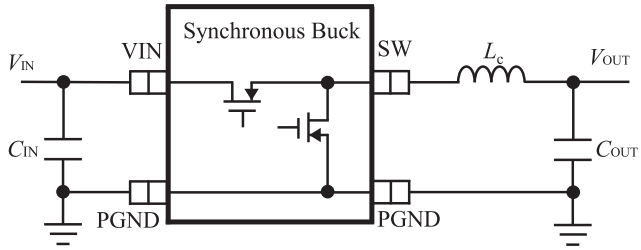

Fig. 3. The buck circuit model measuring efficiency.

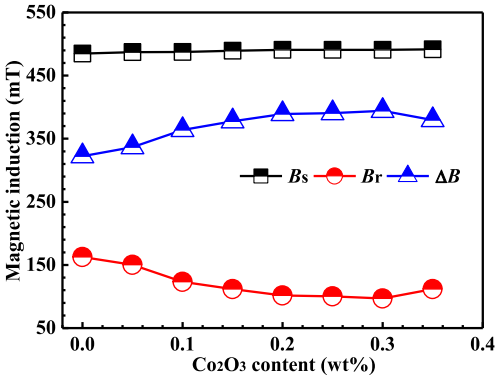

Fig. 4. B_s, B_r, and ΔB of MnZn ferrite cores with different Co_2O_3 content.

capacitance C_{OUT} were both 22 μF, and the input voltage V_{IN} was set at 5 V. The efficiency of the circuit was calculated using the input voltage V_{IN}, input current I_{IN}, output voltage V_{OUT}, and output current I_{OUT}.

III. Results and Discussion

A. B_s, B_r, and ΔB

Saturation induction B_s, remanent induction B_r, and ΔB of the samples with different Co_2O_3 content are shown in Fig. 4. MnZn ferrites are typical spinel structures containing two kinds of sub-lattices: tetrahedral site (A site) and octahedral site (B site), and the magnetic ions Co^{2+} are positioned at the B site [20]–[23]. The molecular magnetic moment $M = |M_B - M_A|$ increases when Co_2O_3 content inceases, where M_A and M_B are total magnetic moments in A and B sites, respectively. Due to the opposite variation trend of B_r, ΔB initially increases and then decreases, with a maximum of 398 mT at 0.30 wt% Co_2O_3. ΔB is generally used to estimate the ability of bearing external magnetic field for ferrite cores [9], [10]. A large ΔB indicates the sample core demands a high external magnetic field to achieve saturation. Therefore, the 0.30 wt% Co_2O_3 sample exhibits the best dc bias superposition characteristic of permeability in preliminarily experiments.

B. DC Bias Superposition Characteristic of Permeability

To determine incremental permeability μ_Δ, ac singal of 1 kHz and 1.9×10^{-3} mT increment of induction is used. The dc bias field varies from 0 to 770 A/m. As shown in Fig. 5(a), incremental permeability μ_Δ of all MnZn ferrite samples shows a tendency of initially increasing and then gradually decreasing. Permeability is closely associated with the magnetization process due to domain wall movement and domain rotation [24]. As presented in Figs. 6 and 7, the average grain size D for all samples is approximately 5 μm. It has been reported that critical size of single-domain state in MnZn ferrites is 3–5 μm [25]. Thus, the studied materials are considered in multi-domain state, because the average grain size of the studied materials is a little bigger than the critical size. When the domain structure in grains transfers from a single-domain to multiple-domain state, domain wall movement gradually dominates the magnetization process [26]–[28]. Therefore, the increasing stage of incremental permeability is induced by relieving domain wall pinning, which can be divided into three parts.

1) When there is no dc bias field, domain walls are pinned by an anisotropy field induced by Co^{2+} ions and other factors, such as pores and stress.
2) When the value of H_{dc} is low, the excitation of H_{dc} promotes domain wall movement, and domain walls can gradually get rid of pinning factors, resulting in an increase in μ_Δ.
3) When H_{dc} increases to a certain value (for instance, 80.2 A/m for 0.30 wt% Co_2O_3 sample), μ_Δ reaches a maximum. The state indicates that the irreversible domain wall movement has merged, as a result of the Barkhausen jumps [29]. As H_{dc} continuously increases, domain walls gradually disappear and become insignificant in the magnetization process, decreasing the incremental permeability [30].

With an increase in Co_2O_3 content, $H_{\mu max}$ (defined as the value of H_{dc} corresponding to the maximum of incremental permeability) initially increases and then decreases, with a maximum of 80.2 A/m at 0.30 wt% Co_2O_3. Details of $H_{\mu max}$ are presented in Fig. 7. Essentially, $H_{\mu max}$ can equal the critical field H_0 for irreversible domain wall movement. The qualitative expression of H_0 is as follows [31]:

$$H_0 \propto K_1/\mu_0 M_S \tag{2}$$

where K_1 represents magneto-crystalline anisotropy constant, μ_0 represents vacuum permeability, and M_s represents the saturation magnetization. The variation in $H_{\mu max}$ can be interpreted in two ways. On one hand, the Co^{2+} ions, which prefer to occupy B sites in MnZn ferrites, can induce a local anisotropy field and pin domain wall. Therefore, large H_{dc} is needed to ensure the domain walls to move in the constraint of local anisotropy field. On the other hand, an increase in M_s can lead to a decrease in $H_{\mu max}$ when the Co_2O_3 content exceeds 0.30 wt%.

The dc bias superposition characteristic of permeability can also be assessed by μ_Δ/μ, where μ is permeability without H_{dc}. The value of μ_Δ/μ reflects the varying ratio of permeability. The 0.30 wt% Co_2O_3 sample has the largest $H_{\mu max}$ as mentioned before, and the smallest decay ratio of permeability to approximately 150 A/m as shown in Fig. 5(b). Therefore, the 0.30 wt% Co_2O_3 sample can bear larger dc bias field, and its permeability is more stable under dc bias field compared with other samples. Through the abovementioned analysis, theoretically the critical field H_0 is responsible for the dc bias superposition characteristic of permeability, which can be improved by increasing the magneto-crystalline anisotropy constant and reducing saturation magnetization.

To better understand the influence of the dc bias field on the magnetization process, complex permeability of 0.20 wt% Co_2O_3 sample under different dc bias fields is measured (see Fig. 8). When H_{dc} is within $H_{\mu max}$, the permeability spectra indicates a normal relaxation type, and both the domain wall motion and domain rotation contribute to incremental permeabitlity. When H_{dc} is beyond $H_{\mu max}$, the pinning effect on domain walls gradually weakens, and the resonant effect of the

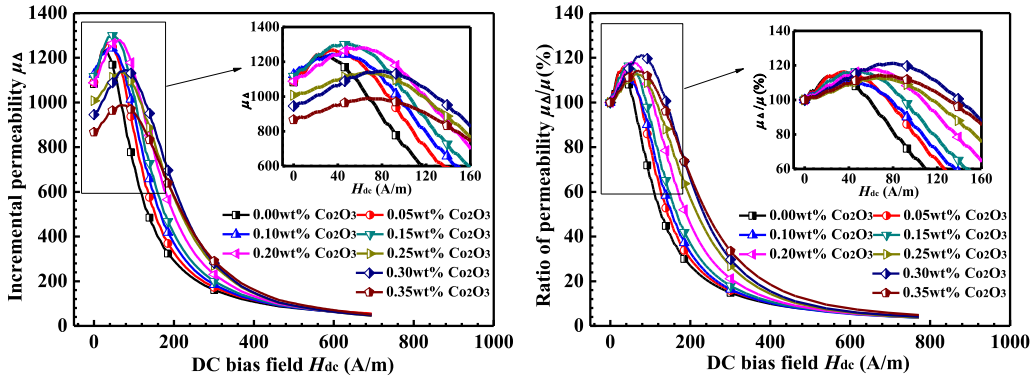

(a) (b)

Fig. 5. (a) Incremental permeability μ_Δ and (b) μ_Δ/μ versus $H_{\rm dc}$ in MnZn ferrite cores with various Co_2O_3 content.

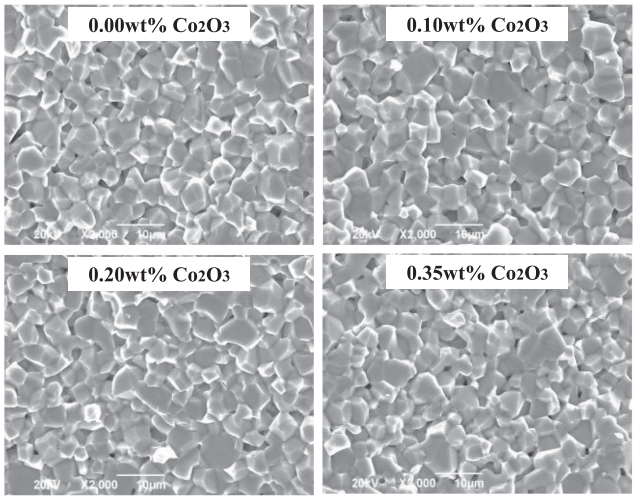

Fig. 6. SEM micrographs of MnZn ferrite cores with various Co_2O_3 content.

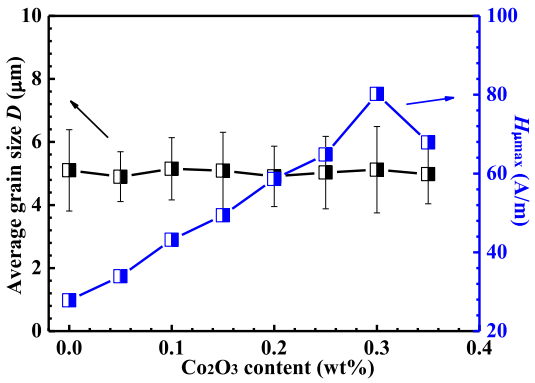

Fig. 7. Average grain size D and $H_{\mu\max}$ of MnZn ferrite cores with different Co_2O_3 content.

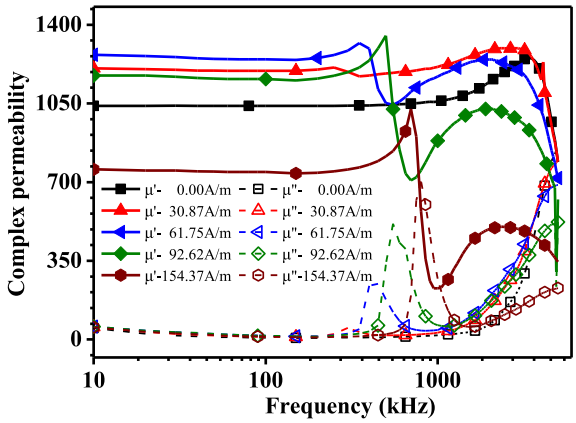

Fig. 8. Complex permeability of MnZn ferrite with 0.20 wt% Co_2O_3 under different dc bias fields.

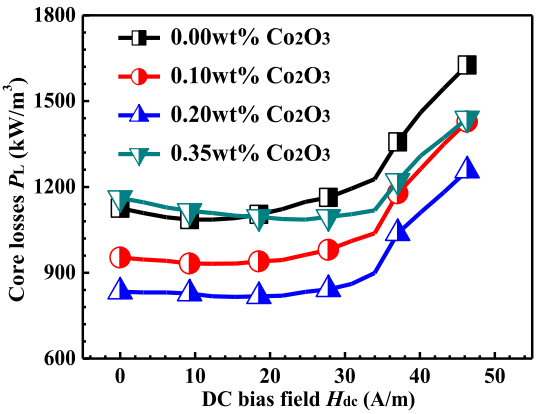

Fig. 9. The variation of core losses with $H_{\rm dc}$ for MnZn ferrite cores at 100 kHz, 200 mT, and 25 °C.

domain walls is shown obviously, resulting in a sharp drop in real part of complex permeability μ' and a peak in imaginary part of complex permeability μ''. An increase in $H_{\rm dc}$ results in the peak of μ'' shifting to higher frequency due to the increase in stiffness of the domain walls [32].

C. Dependence of Core Losses and $H_{\rm dc}$

The application frequency of MnZn ferrites varies from kilohertz to megahertz. In this paper, the dc bias superposition characteristic of core losses is tested using two different testing conditions, at a low frequency of 100 kHz 200 mT and a high frequency of 1 MHz 50 mT.

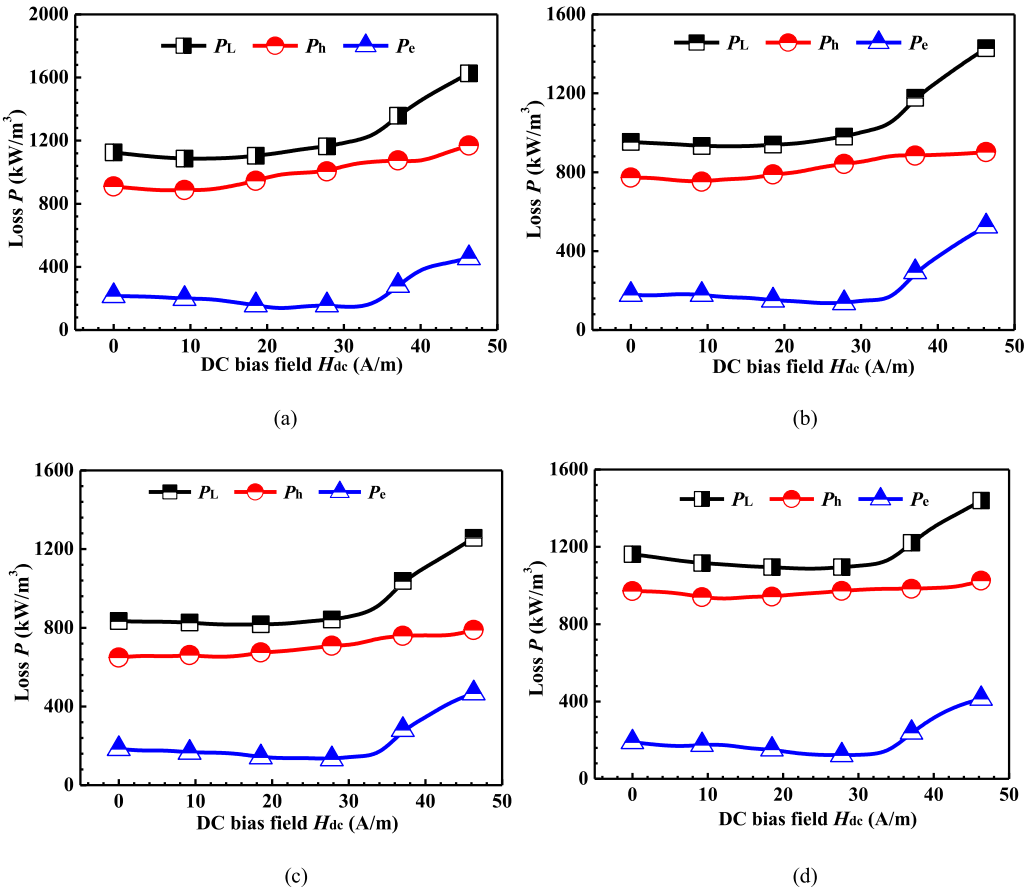

Fig. 10. $P_{\rm L}$, $P_{\rm h}$, and $P_{\rm e}$ versus $H_{\rm dc}$ for MnZn ferrite cores with various Co_2O_3 content at 100 kHz, 200 mT, and 25 °C: (a) 0.00 wt% Co_2O_3, (b) 0.10 wt% Co_2O_3, (c) 0.20 wt% Co_2O_3, (d) 0.35 wt% Co_2O_3.

1) Core Losses at 100 kHz, 200 mT, and 25 °C: Fig. 9 shows the dependence of core losses on $H_{\rm dc}$. As $H_{\rm dc}$ increases, an initial decrease followed by a subsequent increase in core losses $P_{\rm L}$ is observed at 100 kHz, 200 mT, and 25 °C. To determine the dc bias superposition characteristic of core losses, comparison between the samples in this paper and MnZn ferrite material N87 (Epcos) is performed. The core losses of N87 start to increase at approximately 10 A/m [17]. However, the core losses for the samples in this paper start to increase at approximately 30 A/m. Therefore, the dc bias superposition characteristic of the samples in this paper is superior to that of N87.

To analyze the physical mechanism of dc bias superposition characteristic of core losses, separation of core losses was performed. Basically, core losses are from three contributors: hysteresis loss $P_{\rm h}$, eddy current loss $P_{\rm e}$, and residual loss $P_{\rm r}$, described in the following expression [18], [33]:

$$P_{\rm L} = P_{\rm h} + P_{\rm e} + P_{\rm r} = W_{\rm h} f + K_{\rm e} B^2 f^2 / \rho + P_{\rm r} \qquad (3)$$

where W_h represents the area of dc *B–H* loop under the same maximum induction, $K_{\rm e}$ represents constant related to eddy current loss, f represents the frequency, B represents the magnetic induction, and ρ represents the resistivity. According to the measured dc *B–H* loop under the same maximum induction, $W_{\rm h}$ was obtained through integral calculus, thereby $P_{\rm h}$ was calculated by multiplying $W_{\rm h}$ with f. Next, $P_{\rm e}$ and $P_{\rm h}$ can be separated by dividing $(P_{\rm L} - P_{\rm h})$ by f

$$(P_{\rm L} - P_{\rm h}) / f = K_{\rm e} B^2 f / \rho + P_{\rm r} / f. \qquad (4)$$

The curve of $(P_{\rm L} - P_{\rm h})/f - f$ was plotted. The slope represents $P_{\rm e}/f$ and the remainder represents $P_{\rm r}/f$ [34]–[36]. The values of $P_{\rm e}$ and $P_{\rm r}$ are calculated by multiplying each part with f. Even though the magnetized volume of ferrite core is changed in different dc bias field, the frequency dependence of loss is the intrinsic characteristic in a fixed dc bias field, which is the key to perform the loss separation. The separation results are shown in Fig. 10.

For all samples investigated, $P_{\rm h}$ constitutes a major part of core losses and the remainder is $P_{\rm e}$. $P_{\rm r}$ is negligible due to the low measurement frequency of 100 kHz [18], [29]. It is noteworthy that an increase in $H_{\rm dc}$ results in an initial decrease in $P_{\rm h}$, which then gradually increases. $P_{\rm h}$ is caused by irreversible domain wall movements and proportional to the area of *B–H* loop W_h. As presented in Fig. 11(a), the value of W_h calculated from *B–H* loops, first decreases and then increases with an increase in $H_{\rm dc}$. Obviously, the variation in W_h is corresponding to that in $P_{\rm h}$, indicating that the effect of dc bias field on $P_{\rm h}$ is through the change of *B–H* loop. Additionally, due to the existence of $H_{\rm dc}$, the toroidal core is already magnetized before the testing signal

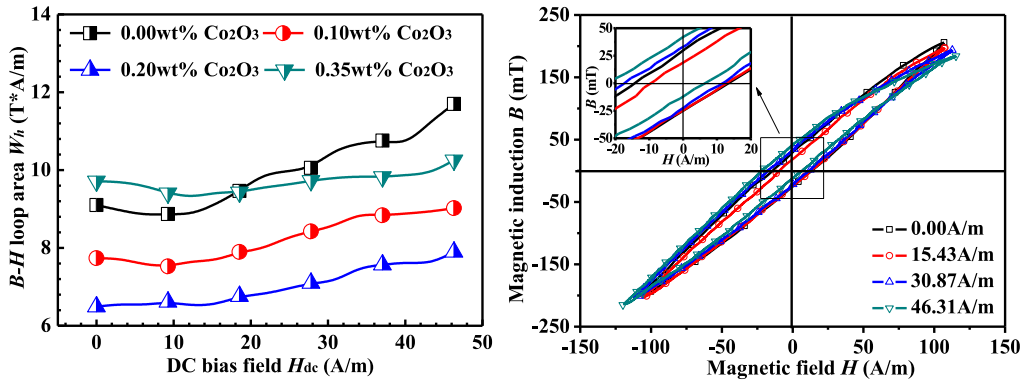

(a) (b)

Fig. 11. (a) The variation of W_h with $H_{\rm dc}$ and (b) dc B–H loops of 0.20 wt% Co_2O_3 sample at 200 mT for various $H_{\rm dc}$.

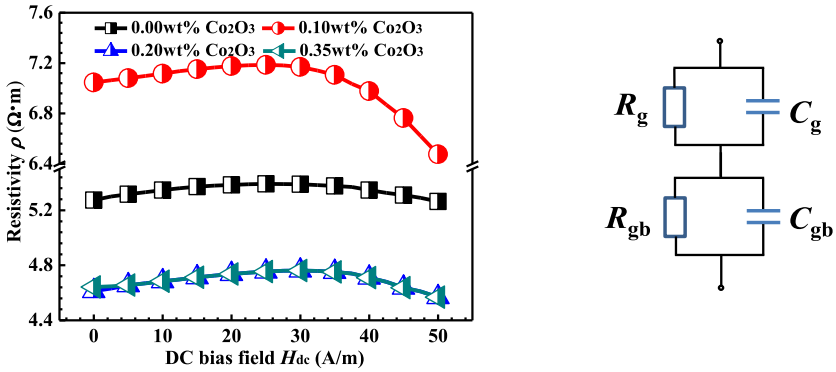

(a) (b)

Fig. 12. (a) Resistivity versus $H_{\rm dc}$ for MnZn ferrite sheets at 100 kHz. (b) The equivalent circuit of microstructure of MnZn ferrites.

is switched on, resulting in the distortion and asymmetry of B–H loop, as shown in Fig. 11(b).

Eddy current loss $P_{\rm e}$ originates from the eddy current when ferrite core locates in ac field, and is inversely proportional to resistivity ρ, as presented in (3). For the interpretation of the variation of $P_{\rm e}$ with $H_{\rm dc}$, the resistivity at 100 kHz is measured and presented in Fig. 12(a). With an increase in $H_{\rm dc}$, resistivity initially increases and then decreases. Theoretically, the heterogeneous microstructure of MnZn ferrites, which consists of grain and grain boundary, can be regarded as an equivalent circuit as shown in Fig. 12(b) [37]. $R_{\rm g}$ and $C_{\rm g}$ represent resistance and capacitance for grain, $R_{\rm gb}$ and $C_{\rm gb}$ represent resistance and capacitance for grain boundary, respectively. At 100 kHz, the conducting process is mainly contributed by electron hopping between Fe^{2+} and Fe^{3+} in grains. This process can be weakened by magneto-resistive effect due to the motion of the electrons under dc bias field being constrained by Lorentz forces. Thus, $R_{\rm g}$ and resistivity increase within 0 to approximately 30 A/m of $H_{\rm dc}$. Sequentially, as $H_{\rm dc}$ increases, a decrease in resistivity occurs due to the capacitive character of the grain boundary. The thickness of the high-resistivity grain boundary is far thinner than the grain size and is approximately in nanometer size [38]. Driven by dc bias field, the electrons aggregate at the grain boundary; thus, the capacitive character of the grain boundary is awoke. When $H_{\rm dc}$ exceeds 30 A/m where $P_{\rm e}$ starts to increase, the electric field generated by the electrons causes quantum charge tunneling across the grain boundary, leading to a decrease in resistivity of grain boundary [39].

2) Core Losses at 1 MHz, 50 mT, and 25 °C: Theoretically, at 100 kHz, 200 mT, and 25 °C, residual loss is insignificant, as shown in Fig. 10. To investigate the effect of dc bias field on residual loss, measurement of high-frequency core losses is necessary and separation of core losses is also performed. Fig. 13 presents the separation results at 1 MHz, 50 mT, and 25 °C. Core losses generally increase monotonically with an increase in $H_{\rm dc}$, with the exception of samples with 0.10 wt% and 0.35 wt% Co_2O_3. As $H_{\rm dc}$ increases, hysteresis loss shows a similar trend at 100 kHz, 200 mT, and 25 °C due to the evolution of B–H loops.

Eddy current loss increases monotonically at 1 MHz, 50 mT, and 25 °C. Resistivity at 1 MHz is measured and a monotonic decrease occurs with an increase in $H_{\rm dc}$ [see Fig. 14(a)]. The literature reports that the resistivity of soft ferrite decreases significantly with increasing frequency [40], as seen in the data in Fig. 14(b). At high-frequency ranges, the capacitive reactance $1/2\pi f C_{\rm gb}$ decreases and $R_{\rm gb}$ becomes close to being

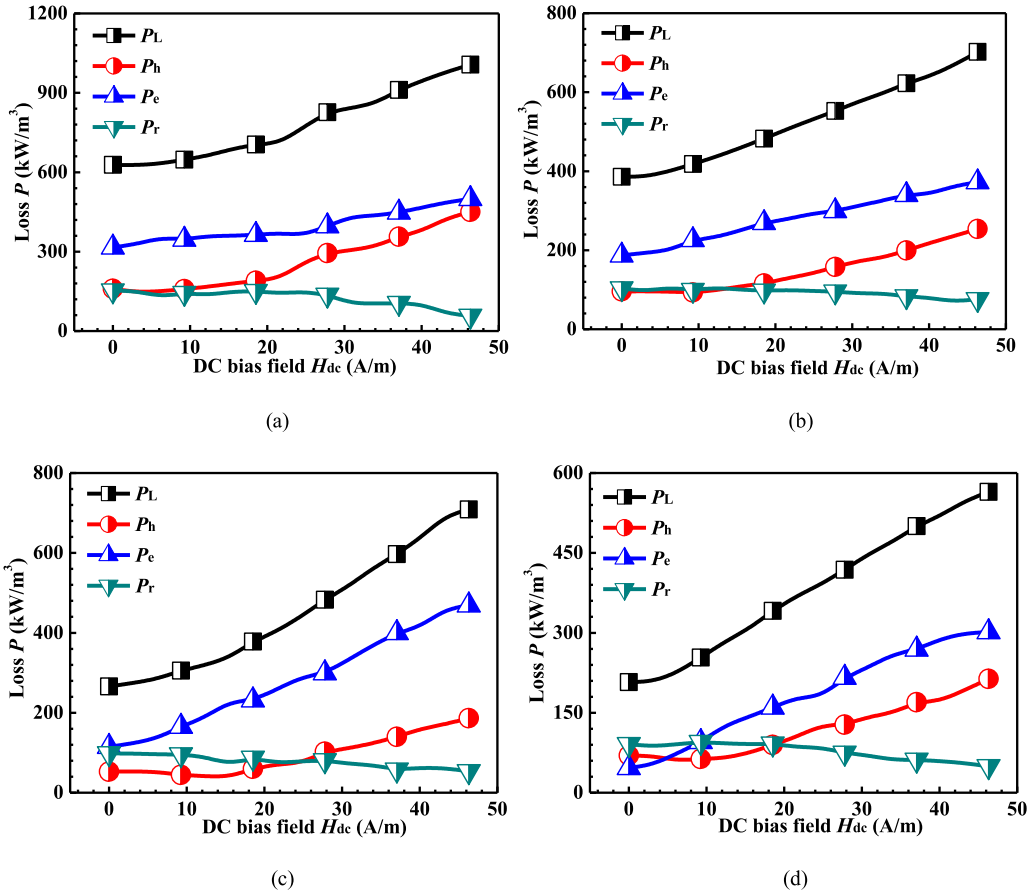

Fig. 13. P_L, P_h, P_e, and P_r versus H_{dc} for MnZn ferrite cores with various Co_2O_3 content at 1 MHz, 50 mT, and 25 °C: (a) 0.00 wt% Co_2O_3, (b) 0.10 wt% Co_2O_3, (c) 0.20 wt% Co_2O_3, (d) 0.35 wt% Co_2O_3.

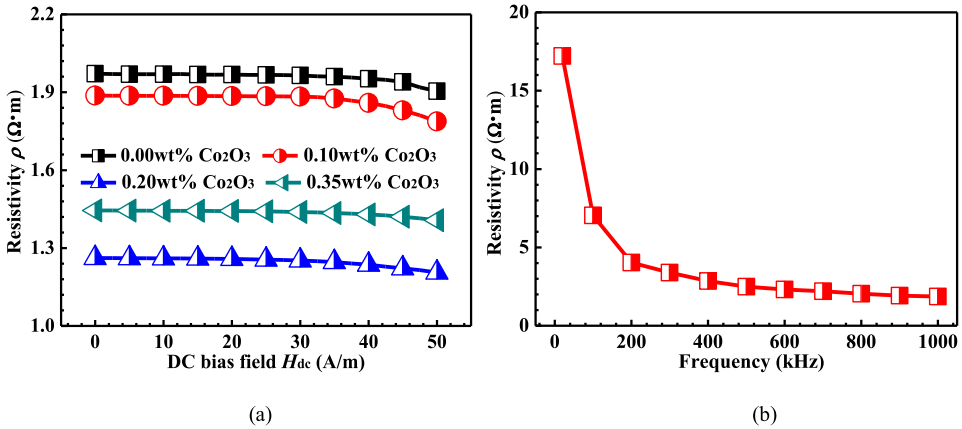

Fig. 14. (a) Resistivity versus H_{dc} at 1 MHz and (b) resistivity versus frequency for MnZn ferrite sheet with 0.20 wt% Co_2O_3 content.

short-circuited, resulting in dramatic decrease in resistivity at the grain boundary. Besides, the electron hopping in grains gets more effortless which prevails over the magneto-resistive effect, resulting in the monotonous variation in resistivity and P_e with an increase in H_{dc} at 1 MHz [41].

Residual loss, related to the resonant phenomenon of domain walls, decreases with an increase in H_{dc}. Although the excitation of H_{dc} promotes the movement of domain walls, the domain walls will gradually disappear as H_{dc} increases [10]. Consequently, the ferrite core easily translates into a single-domain state under dc bias field, leading to a decrease in residual loss [35].

Through abovementioned analysis of dc bias superposition characteristic of core losses, a new thought for tunable dc bias superposition characteristic was proposed: by means of adjusting the contribution of each part of loss, the ferrite core can have

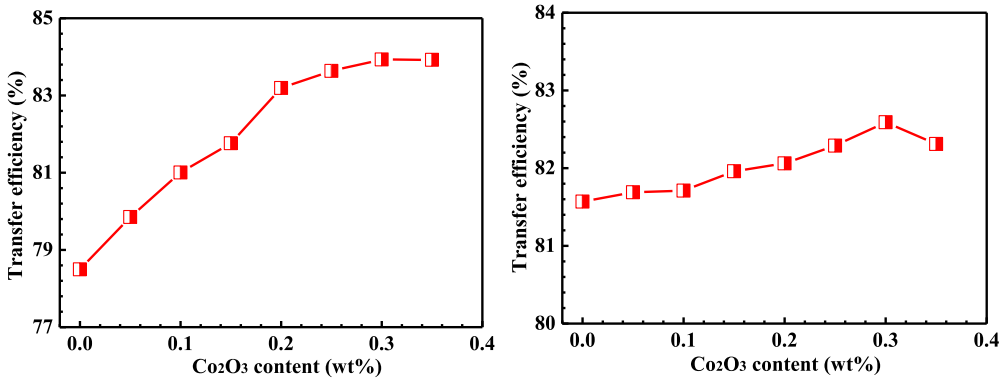

Fig. 15. Efficiency versus Co_2O_3 content at (a) 240 kHz and (b) 1.1 MHz.

low core losses at a certain value of H_{dc}, which is meaningful for improving the efficiency in the power converters.

D. Effect of Co_2O_3 Content Applied to a Buck Circuit

The ferrite cores with varying Co_2O_3 contents are tested in a buck circuit (see Fig. 3) and the efficiency of the circuit is determined. Two different chips with operating frequency of 240 kHz and 1.1 MHz are used.

As presented in Fig. 15, with an increase in Co_2O_3 content, the efficiency of the circuit initially increases and then slightly decreases, at both low (240 kHz) and high (1.1 MHz) frequency, which is in agreement with the variation in core loss outlined in Section III-C. This phenomenon indicates that the reduction of core losses is responsible for increasing efficiency. An optimal Co_2O_3 content of 0.30 wt% with relatively low core losses (150 kW/m^3 at 1 MHz 50 mT 25 °C and 900 kW/m^3 at 100 kHz 200 mT 25 °C) can improves the efficiency of the buck circuit. The variation in efficiency with Co_2O_3 content at 1.1 MHz is insignificant compared to that at 240 kHz. In fact, dissipation in the circuit is related not only to the core losses of ferrite, but also to other factors, such as the loss of MOSFETs and copper. Therefore, at high-frequency range, efficiency does not significantly depend on the Co_2O_3 content due to the relatively small contribution of core losses to the whole dissipation.

IV. Conclusion

This paper investigates the dc bias superposition characteristics in Co_2O_3 doped MnZn ferrites. The results indicate that the MnZn ferrite sample with 0.30 wt% Co_2O_3 has the best dc bias superposition characteristic of permeability, with an initial permeability μ_i of 945. Interestingly, core losses P_L at 100 kHz, 200 mT, and 25 °C are found to initially decrease and then increase as H_{dc} increases. Correspondingly, core losses P_L at 1 MHz, 50 mT, and 25 °C increase monotonically with an increase in H_{dc}. This phenomenon of core losses suggests a novel application for MnZn ferrite cores working under dc bias superposition conditions. This is shown in a buck converter in which the 0.30 wt% Co_2O_3 sample improves the efficiency of the converter.

References

[1] M. A. Ahmed, K. E. Rady, and M. S. Shams, "Enhancement of electric and magnetic properties of Mn-Zn ferrite by Ni-Ti ions substitution," *J. Alloys Compound*, vol. 622, pp. 269–275, Feb. 2015.

[2] J. Töpfer and A. Angermann, "Complex additive systems for Mn-Zn ferrites with low power loss," *J. Appl. Phys.*, vol. 117, Apr. 2015, Art. no. 17A504.

[3] D. Liu *et al.*, "MnZn power ferrite with high B_s and low core loss," *Ceram. Int.*, vol. 42, pp. 9152–9156, May. 2016.

[4] J. Reinert, A. Brockmeyer, and R. W. A. A. De Doncker, "Calculation of losses in ferro- and ferromagnetic materials based on the modified Steinmetz equation," *IEEE Trans. Ind. Appl.*, vol. 37, no. 4, pp. 1055–1061, Jul. 2001.

[5] C. A. Baguley, B. Carsten, and U. K. Madawala, "An investigation into the impact of DC bias conditions on ferrite core losses," in *Proc 33rd Annu. Conf. IEEE Ind. Electron. Soc.*, Nov. 2007, pp. 1408–1413.

[6] H. Kosai, Z. Turgut, and J. Scofield, "Experimental investigation of DC-bias related core losses in a boost inductor," *IEEE Trans. Magn.*, vol. 49, no. 7, pp. 4168–4171, Jul. 2013.

[7] Y. Liu and S. He, "Development of low loss Mn-Zn ferrite working at frequency higher than 3 MHz," *J. Magn. Magn. Mater.*, vol. 320, pp. 3318–3322, Dec. 2008.

[8] Y. Liu and S. He, "Development of high DC-bias Mn-Zn ferrite working at frequency higher than 3 MHz," *J. Alloys Compound*, vol. 489, pp. 523–529, Jan. 2010.

[9] X. Tang, H. Zhang, H. Su, Z. Zhong, and F. Bai, "Influence of microstructure on the DC-bias-superposition characteristics of NiZn ferrite," *IEEE Trans. Magn.*, vol. 47, pp. 4332–4335, Oct. 2011.

[10] S. Yan, L. Dong, Z. Chen, X. Wang, and Z. Feng, "The effect of the microstructure on the DC-bias superposition characteristic of NiCuZn ferrite," *J. Magn. Magn. Mater.*, vol. 353, pp. 47–50, Mar. 2014.

[11] T. Kawano, A. Fujita, and S. Gotoh, "Analysis of power loss at high frequency for MnZn ferrites," *J. Appl. Phys.*, vol. 87, pp. 6214–6216, May 2000.

[12] C. A. Baguley, U. K. Madawala, and B. Carsten, "A new technique for measuring ferrite core loss under DC bias conditions," *IEEE Trans. Magn.*, vol. 44, no. 11, pp. 4127–4130, Nov. 2008.

[13] C. A. Baguley, U. K. Madawala, and B. Carsten, "Unusual effects measured under DC bias conditions on MnZn ferrite material," *IEEE Trans. Magn.*, vol. 45, no. 9, pp. 3215–3222, Sep. 2009.

[14] C. A. Barguley, B. Carsten, and U. K. Madawala, "The effect of DC bias conditions on ferrite core losses," *IEEE Trans. Magn.*, vol. 44, no. 2, pp. 246–252, Feb. 2008.

[15] M. Mu, Y. Su, Q. Li, and F. C. Lee, "Magnetic characterization of low temperature co-fired ceramic (LTCC) ferrite materials for high frequency power converters," in *Proc. Energy Convers. Congr. Expo.*, Sep. 2011, pp. 2133–2138.

[16] M. Mu, F. Zheng, Q. Li, and F. C. Lee, "Finite element analysis of inductor core loss under DC bias conditions," *IEEE Trans. Power Electron.*, vol. 28, no. 9, pp. 4414–4421, Sep. 2013.

[17] J. Mühlethaler, J. Biela, J. W. Kolar, and A. Ecklebe, "Core losses under the DC bias condition based on Steinmetz parameters," *IEEE Trans. Power Electron.*, vol. 27, no. 2, pp. 953–963, Feb. 2012.

[18] A. Fujita and S. Gotoh, "Temperature dependence of core loss in co-substituted MnZn ferrites," *J. Appl. Phys.*, vol. 93, no. 10, pp. 7477–7479, May 2003.

[19] L. Li, Z. Lan, Z. Yu, and K. Sun, "Influence of Fe_2O_3 stoichiometry on initial permeability and temperature dependence of core loss in MnZn ferrites," *IEEE Trans. Magn.*, vol. 44, no. 1, pp. 13–16, Jan. 2008.

[20] W. D. Yang and Y. G. Wang, "Effects of TiO_2 and Co_2O_3 combination additions on the elemental distribution and electromagnetic properties of Mn-Zn power ferrites," *J. Magn. Magn. Mater.*, vol. 384, pp. 13–17, Jun. 2015.

[21] L. Li, Z. Lan, Z. Yu, K. Sun, and Z. Xu, "Effects of co-substitution on wide temperature ranging characteristic of electromagnetic properties in MnZn ferrites," *J. Alloys Compound*, vol. 476, pp. 755–759, May 2009.

[22] Q. Zhang, P. Zheng, L. Zheng, J. Zhou, and H. Qin, "Effect of co-substitution on the structure and magnetic properties of MnZn power ferrite," *J. Electroceram.*, vol. 32, pp. 230–233, May 2014.

[23] C. F. Zhang, X. C. Zhong, H. Y. Yu, Z. W. Liu, and D. C. Zeng, "Effects of cobalt doping on the microstructure and magnetic properties of Mn-Zn ferrites prepared by the co-precipitation method," *Physica B: Condens. Matter*, vol. 404, pp. 2327–2331, Aug. 2009.

[24] H. Liu *et al.*, "Study on the contribution of magnetization mechanisms in NiZn ferrites," *IEEE Trans. Magn.*, vol. 51, no. 11, pp. 1–4, Nov. 2014.

[25] P. J. van der Zaag, "New views on the dissipation in soft magnetic ferrites," *J. Magn. Magn. Mater.*, vol. 196–197, pp. 315–319, May 1999.

[26] C. A. Stergiou and V. Zaspalis, "Analysis of the complex permeability of NiCuZn ferrites up to 1 GHz with regard to Cu content and sintering temperature," *Ceram. Int.*, vol. 40, pp. 357–366, Jan. 2014.

[27] N. Jiang, Y. Yang, Y. Zhang, J. Zhou, P. Liu, and C. Deng, "Influence of zinc concentration on structure, complex permittivity and permeability of Ni-Zn ferrites at high frequency," *J. Magn. Magn. Mater.*, vol. 401, pp. 370–377, Mar. 2016.

[28] K. Sun *et al.*, "Contribution of magnetization mechanisms in nickel-zinc ferrites with different grain sizes and its temperature relationship," *Mater. Chem. Phys.*, vol. 175, pp. 131–137, Jun. 2016.

[29] K. Sun *et al.*, "Cation distribution and magnetic property of Ti/Sn-substituted manganese-zinc ferrites," *J. Alloys Compound*, vol. 650, pp. 363–369, Nov. 2015.

[30] P. Pan and N. Zhang, "Magnetodielectric effect of Mn-Zn ferrite at resonant frequency," *J. Magn. Magn. Mater.*, vol. 416, pp. 256–260, Oct. 2016.

[31] D. C. Jiles, "Dynamics of domain magnetization and the Barkhausen effect," *Czechoslovak J. Phys.*, vol. 50, no. 8, pp. 893–988, Apr. 2000.

[32] T. Tsutaoka, T. Nakamura, and K. Hatakeyama, "Magnetic field effect on the complex permeability spectra in a Ni-Zn ferrite," *J. Appl. Phys.*, vol. 82, pp. 3068–3071, Sep. 1997.

[33] K. Sun *et al.*, "Temperature and frequency characteristics of low-loss MnZn ferrite in a wide temperature range," *J. Appl. Phys.*, vol. 109, May 2011, Art. no. 106103.

[34] D. Stoppels, "Developments in soft magnetic power ferrites," *J. Magn. Magn. Mater.*, vol. 160, pp. 323–328, Jul. 1996.

[35] W. H. Jeong, Y. H. Han, and B. M. Song, "Effects of grain size on the residual loss of MnZn ferrites," *J. Appl. Phys.*, vol. 91, pp. 7619–7621, May. 2002.

[36] K. Sun, Z. Lan, Z. Yu, L. Li, X. Nie, and Z. Xu, "Analysis of losses in NiO doped MnZn ferrites," *J. Alloys Compound*, vol. 468, pp. 315–320, Jan. 2009.

[37] C. G. Koops, "On the dispersion of resistivity and dielectric constant of some semiconductors at audio frequencies," *Phys. Rev.*, vol. 83, pp. 121–124, Jul. 1951.

[38] A. H. Qureshi, "The influence of Hafnia and impurities (CaO/SiO_2) on the microstructure and magnetic properties of Mn-Zn ferrites," *J. Cryst. Growth*, vol. 286, pp. 365–370, Jan. 2006.

[39] W. A. Roshen, "Magnetic loss in soft ferrites," *J. Appl. Phys.*, vol. 101, May 2007, Art. no. 09M522.

[40] C. S. Liu and J. M. Wu, "High-power-use Mn-Zn ferrites with monodomain structure prepared by low-temperature sintering," *J. Appl. Phys.*, vol. 79, pp. 5432–5434, 1996.

[41] M. S. Khandekar, R. C. Kambale, J. Y. Patil, Y. D. Kolekar, and S. S. Suryavanshi, "Effect of calcination temperature on the structural and electrical properties of cobalt ferrite synthesized by combustion method," *J. Alloys Compound*, vol. 509, pp. 1861–1865, Feb. 2011.

Guohua Wu received the B.S. degree from the School of Micro Electronics and Solid State Electronics, University of Electronic Science and Technology of China, Chengdu, China, in 2010. He is currently working toward the Ph.D. degree at the School of Materials and Energy, University of Electronic Science and Technology of China. He is now majoring in MnZn power ferrite material applied in high-frequency range and devoting himself in studying the physic mechanism of high-frequency core losses.

Zhong Yu received the B.S. degree from Department of Macromolecular Science, Fudan University, Shanghai, China, in 1993, the M.S. and Ph.D. degrees from the School of Micro Electronics and Solid State Electronics, University of Electronic Science and Technology of China, Chengdu, China, in 1998 and 2009, respectively.

From 1993 to 1995, he was an Engineer with the China Academy of Engineering Physics. From 2010 to 2017, he worked as a Full Professor with the School of Micro Electronics and Solid State Electronics, University of Electronic Science and Technology of China. Since 2018, he has been a Full Professor with the School of Materials and Energy, University of Electronic Science and Technology of China. His research interests include advanced magnetic material, magnetic thin film, and magnetic component.

Ke Sun (M'xx) received the B.S. degree from the College of Chemical Engineering, Guizhou University, Guizhou, China, in 2003, the M.S. and Ph.D. degrees from the School of Micro Electronics and Solid State Electronics, University of Electronic Science and Technology of China, Chengdu, China, in 2006 and 2009, respectively.

From 2008 to 2009, he worked on the research of microwave/millimeter wave magnetic thin film and component with the Department of Physics, Colorado State University, Fort Collins, CO, USA. From 2016 to 2017, he worked as a Full Professor with the School of Micro Electronics and Solid State Electronics, University of Electronic Science and Technology of China. Since 2018, he has been a Full Professor with the School of Materials and Energy, University of Electronic Science and Technology of China. His research interests include soft magnetic materials and devices, magnetic films and integrated devices, and microwave ferrites and devices.

Rongdi Guo received the B.S. and Ph.D. degrees from the School of Micro Electronics and Solid State Electronics, University of Electronic Science and Technology of China, Chengdu, China, in 2009 and 2017, respectively.

From 2014 to 2016, he was engaged in the research of microwave/millimeter-wave soft magnetic thick film deposition and magnetic modulation microwave/millimeter-wave device design with the Department of Computer and Electronic Engineering, Northeastern University, Boston, MA, USA. His research interests include ferrite bulk material, thick film, and microwave/millimeter wave device design and fabrication.

Bo Wang received the B.S. and M.S. degrees from the School of Micro Electronics and Solid State Electronics, University of Electronic Science and Technology of China, Chengdu, China, in 2011 and 2014, respectively. He majored in MnZn power ferrite material applied in low-frequency and wide temperature range.

Xiaona Jiang received the B.S. degree from the Wuhan University of Technology, Wuhan, China, in 2000, and the M.S. and Ph.D. degrees from the School of Micro Electronics and Solid State Electronics, University of Electronic Science and Technology of China, Chengdu, China, in 2005 and 2012, respectively.

From 2016 to 2017, she was engaged in the research of ferrite material with Northeastern University, Boston, MA, USA. Her research interests include ferrite bulk material and microwave/millimeter wave device design.

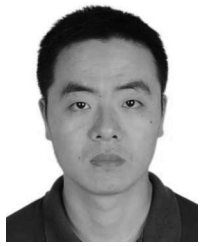

Lezhong Li received the B.S. degree from Yantai Normal University, Shandong, China, in 2004, and the Ph.D. degree from the School of Micro Electronics and Solid State Electronics, University of Electronic Science and Technology of China, Chengdu, China, in 2009.

Since 2019, he has been a Full Professor with the College of Optoelectronic Engineering, Chengdu University of Information Technology, Chengdu. He has been engaging on microwave magnetic materials and components.

Zhongwen Lan received the B.S. and M.S. degrees from the School of Information Materials, University of Electronic Science and Technology of China, Chengdu, China, in 1983 and 1986, respectively.

From 2002 to 2017, he worked as a Full Professor with the School of Micro Electronics and Solid State Electronics, University of Electronic Science and Technology of China. Since 2018, he has been a Full Professor with the School of Materials and Energy, University of Electronic Science and Technology of China. He has been engaged in magnetic material and devices since 1983.

Prof. Lan is the member of Applied Magnetism Branch, Chinese Society of Electronics, and the member of Chinese Standardization Committee of Magnetic Elements and Ferrite Materials.